Discovery of *N*-Phenyl-4-(thiazol-5-yl)pyrimidin-2-amine Aurora Kinase Inhibitors

Shudong Wang,[†] Carol A. Midgley, Frederic Scaërou, Joanna B. Grabarek, Gary Griffiths, Wayne Jackson, George Kontopidis,[‡] Steven J. McClue, Campbell McInnes,[§] Christopher Meades, Mokdad Mezna, Andy Plater, Iain Stuart, Mark P. Thomas, Gavin Wood, Rosemary G. Clarke, David G. Blake, Daniella I. Zheleva,* David P. Lane, Robert C. Jackson, David M. Glover, and Peter M. Fischer*,[†]

Cyclacel Ltd., 1 James Lindsay Place, Dundee DD1 5JJ, Scotland, U.K. [†]School of Pharmacy and Centre for Biomolecular Sciences, University of Nottingham, University Park, Nottingham NG7 2RD, U.K. [‡]Biochemistry Laboratory, Veterinary School, University of Thessaly, Karditsa 43100, Greece. [§]South Carolina College of Pharmacy, CLS 514, 715 Sumter Street, University of South Carolina, Columbia, South Carolina 29208.

Through cell-based screening of our kinase-directed compound collection, we discovered that a subset of *N*-phenyl-4-(thiazol-5-yl)pyrimidin-2-amines were potent cytotoxic agents against cancer cell lines, suppressed mitotic histone H3 phosphorylation, and caused aberrant mitotic phenotypes. It was subsequently established that these compounds were in fact potent inhibitors of aurora A and B kinases. It was shown that potency and selectivity of aurora kinase inhibition correlated with the presence of a substituent at the aniline para-position in these compounds. The anticancer effects of lead compound 4-methyl-5-(2-(4-morpholinophenylamino)pyrimidin-4-yl)thiazol-2-amine (**18**; K_i values of 8.0 and 9.2 nM for aurora A and B, respectively) were shown to emanate from cell death following mitotic failure and increased polyploidy as a consequence of cellular inhibition of aurora A and B kinases. Preliminary in vivo assessment showed that compound **18** was orally bioavailable and possessed anticancer activity. Compound **18** (CYC116) is currently undergoing phase I clinical evaluation in cancer patients.

Introduction

The aurora kinases are a family of serine−threonine kinases that interact with components of the mitotic apparatus and that regulate aspects of centrosome maturation, bipolar spindle assembly, chromosome segregation, and cytokinesis (see refs 1 and 2 for recent reviews). Three human aurora kinases have been identified, and these are designated A, B, and C. In interphase, aurora A localizes to the centrosomes, where it is required for their maturation and separation, thereby promoting mitotic entry and spindle assembly. In mitosis, aurora A associates with the spindle poles and is involved in both centrosomal and acentrosomal spindle assembly. Aurora B is a component of the chromosome passenger complex and localizes to the centromeres in prometaphase, then relocating to the spindle midzone at anaphase. It has functions associated with histone phosphorylation and chromatin condensation in prophase, chromosome alignment and segregation, and the regulation of a mitotic checkpoint at metaphase and also has a role in cytokinesis. Aurora C has similar functions as aurora B; it is highly expressed in the testis but is also present at a low level in other tissues.[3]

Human aurora A was first isolated as the product of the BTAK (breast tumor amplified kinase, also known as STK15) gene on chromosome 20q13.3, a region that is frequently amplified in primary breast tumors, colorectal cancers, and many cancer cell lines, including those of breast, ovarian, colon, prostate, neuroblastoma, and cervical origin (reviewed in refs 4 and 5). Aurora A has also been identified as a colon-cancer-associated kinase that is overexpressed in more than 50% of primary colorectal cancers.[6,7] Overexpression of aurora A contributes to genetic instability and tumorigenesis by disrupting the proper assembly of the mitotic checkpoint complex.[8] In addition, this kinase is a key regulatory component of the p53 pathway and its overexpression leads to an increase in p53 degradation, which again facilitates oncogenic transformation.[9] However, despite the fact that certain cells are transformed upon forced aurora A overexpression in vitro, it remains controversial if aurora A is a true oncogene.[10,11] Aurora A overexpression has also been shown to be able to induce resistance to tubulin-disrupting agents, such as paclitaxel, by overriding the mitotic spindle checkpoint.[12] Conversely, synergy between genetic aurora A suppression and the cytotoxicity of taxanes has been demonstrated.[13]

As with aurora A, high-level expression of aurora B in model systems has been linked to chromosome instability.[14,15] In contrast to aurora A, however, the chromosomal region encoding aurora B (AURKB locus 17p13.1) does not generally appear to be amplified in tumors, with the notable exception of non-small-cell lung cancers.[4,16] Nevertheless, aurora B kinase has been found to be strongly expressed in many tumor types and expression levels often correlated with disease state or outcome.[4] A systematic analysis of expression levels of aurora A, B, and C mRNA in multiple primary tumor samples revealed that aurora A and B, but not aurora C, were often significantly overexpressed when compared with normal

*To whom correspondence should be addressed. For D.I.Z.: phone, +44-1382-206062; fax, +44-1382-206067; e-mail: dzheleva@cyclacel.com. For P.M.F. (chemistry): phone, +44-115-8466242; fax, +44-115-9513412; e-mail: peter.fischer@nottingham.ac.uk.
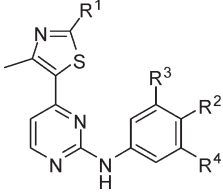
cells and that aurora A and B overexpression was frequently concurrent.[17]

Repression of aurora A by genetic means delayed mitotic entry in human cancer cells,[18] while overexpression of wild-type aurora A compromised spindle checkpoint function and inhibited cytokinesis, leading to centrosome amplification, a characteristic feature of many cancer cells.[19] Exogenous overexpression of aurora B, on the other hand, caused chromosome separation defects during mitosis, while an inhibitory antibody against aurora B prevented efficient chromosome congression and allowed cells to escape spindle checkpoint arrest in the presence of microtubule-inhibiting drugs and to exit mitosis without completing anaphase or cytokinesis.[20]

Direct comparison of the aurora A and B RNA interference phenotypes in cancer cells confirmed that these are distinct but that concurrent suppression resulted predominantly in the aurora B phenotype,[21,22] indicating that inactivation of aurora B may bypass the requirement for aurora A in mitosis.[23] Similarly, some small-molecule ATP-binding site inhibitors (refer to ref 24 for a recent review) do not distinguish between aurora A and B kinases and inhibit both kinases in cells; e.g., the well-documented aurora kinase inhibitors (*Z*)-*N*-(2-oxo-3-(phenyl(4-(piperidin-1-ylmethyl)phenylamino)methylene)-indolin-5-yl)ethanesulfonamide (hesperadin)[25] and *N*-(4-(6-methoxy-7-(3-morpholinopropoxy)quinazolin-4-ylamino)-phenyl)benzamide (ZM447439),[26] as well as the clinical compounds *N*-(4-(4-(5-methyl-1*H*-pyrazol-3-ylamino)-6-(4-methylpiperazin-1-yl)pyrimidin-2-ylthio)phenyl)cyclopropane-carboxamide (MK-0457, VX-680)[27] and (*R*)-I-(5-(2-methoxy-2-phenylacetyl)-1,4,5,6-tetrahydropyrrolo[3,4-*c*]pyrazol-3-yl)-4-(4-methylpiperazin-1-yl)benzamide (PHA-739358),[28] invariably exhibited terminal phenotypes that are more consistent with aurora B rather than aurora A inhibition, i.e. chromosome misalignments, multinucleation, and polyploidy as a consequence of cytokinesis failure.[17,23,29−31] Small-molecule inhibitors selective for aurora A, such as (*E*)-4-(9-chloro-7-(2,6-difluorophenyl)-5*H*-benzo[*c*]pyrimido[4,5-*e*]azepin-2-ylamino)benzoic acid (MLN8054),[22] and for aurora B, e.g., 5-[[7-[3-[ethyl[2-(phosphonooxy)ethyl]amino]propoxy]-4-quinazolinyl]amino]-*N*-(3-fluorophenyl)-1*H*-pyrazole-3-acetamide (AZD1152),[32] have also entered the clinic. Reportedly the former compound is ~40-fold selective for aurora A vs B; at low concentrations it was reported to cause accumulation of cells in G2/M and spindle defects, resulting in apoptotic cell death, whereas at higher concentrations, where aurora B inhibition became significant, loss of cell viability due to polyploidy as a result of mitotic and cytokinesis failure was observed.[22] In a separate report, however, the terminal phenotype of cell treatment with concentrations of this compound that blocked aurora A but not aurora B activity was nevertheless shown to be induction of polyploidy.[33] It thus still remains uncertain how exactly aurora A and B pan- or monospecific inhibitors induce tumor cell death and which type of inhibitor will be preferable from a therapeutic viewpoint.

Table 1. Structures of Kinase Inhibitor Compounds Used in This Study

compd	R^1	R^2	R^3	R^4
9	NH$_2$	H	NO$_2$	H
10	Me	NMe$_2$	H	H
11	Me	NHMe	H	H
12	Me	NH$_2$	H	H
13	Me	OMe	OMe	OMe
14	NHMe	OMe	OMe	OMe
15	NHEt	OMe	OMe	OMe
16	NHEt	CH$_2$NHAc	H	H
17	Me	morpholin-1-yl	H	H
18	NH$_2$	morpholin-1-yl	H	H
19	NHMe	morpholin-1-yl	H	H
20	NHEt	morpholin-1-yl	H	H
21	NH$_2$	4-acetylpiperazin-1-yl	H	H
22	NHMe	4-acetylpiperazin-1-yl	H	H
23	Me	4-acetyl-piperazin-1-yl	H	H
24	Me	4-(methylsulfonyl)piperazin-1-yl	H	H

We have been using a series of cell-based assays to classify and characterize our kinase-directed *N*,4-bis(aryl)pyrimidin-2-amine compounds.[34−38] In this way we identified a series of cyclin-dependent kinase (CDK^a) inhibitors that block RNA polymerase II (RNAPII) dependent transcription.[39] These compounds were found to reduce mitotic index, to increase p53 protein levels, and to induce cellular apoptosis in cancer cells.[39,40] However, we also observed a structurally closely related but mechanistically distinct subset of compounds with similar antiproliferative activities but quite different effects on cell cycle progression than the transcriptional CDK inhibitors. These compounds displayed pronounced mitotic phenotypes and caused polyploidy in cancer cell lines. Here we describe the discovery and characterization of these compounds and how they were identified as potent ATP-competitive aurora kinase A and B inhibitors.

Chemistry

The general chemistry for the synthesis of *N*-phenyl-4-(thiazol-5-yl)pyrimidin-2-amine derivatives (Table1) was adapted from the method described previously[36] and is outlined in Scheme 1. Briefly, 5-acetylthiazoles **3** were prepared from the appropriate thioureas **2** and 3-chloro-2,4-pentadione **1** and were converted to the corresponding enaminones **4** by heating in *N*,*N*-dimethylformamide dimethyl acetal.[41] The enaminones were then condensed with the appropriate phenylguanidines **8** at elevated temperature in alcoholic alkali to form the desired pyrimidines **9−24**. The phenylguanidines **8** were derived from the corresponding anilines **7** by treatment with aqueous cyanamide.[36] To prepare 1-(4-morpholinophenyl)guanidine **8g** and 1-(4-(4-substituted piperazin-1-yl)phenyl)guanidines **8h** and **8i**, 4-fluoronitrobenzene **5** was used as the starting material, which was treated with morpholine or piperazine derivatives in the presence of base to afford the corresponding substituted nitrobenzenes **6**.[42] Reduction of the nitro group provided the anilines **7g−i**.

Scheme 1[a]
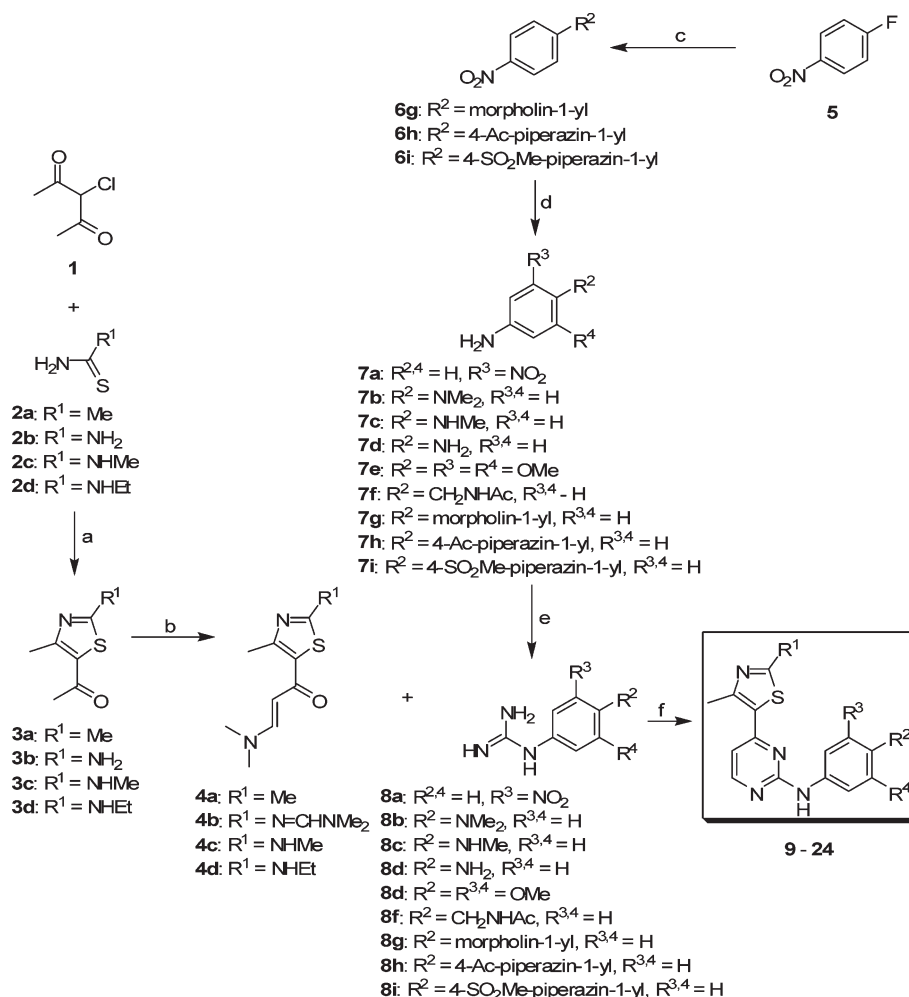
[a] Reagents: (a) MeOH, room temp, 4−6 h; (b) *N,N*-dimethylformamide dimethylacetal, Δ, 12−16 h; (c) morpholine, 4-acetylpiperazine, or 4-(methylsulfonyl)piperazine, K_2CO_3, DMF; (d) H_2, Pd(C), or Fe, AcOH, EtOH, room temp, 12−15 h; (e) aq H_2NCN, HCl or HNO_3, EtOH, Δ, 12−16 h; (f) NaOH, 2-methoxyethanol, Δ, 12−24 h; or microwave, 150 °C, 20−30 min.

Results and Discussion

Discovery of Aurora Kinase Inhibitor Compounds. Upon testing our collection of several hundred *N*,4-bis(aryl)pyrimidin-2-amine kinase inhibitor compounds[34−38] in cell-based screens, we discovered that a subset of *N*-phenyl-4-(thiazol-5-yl)pyrimidin-2-amines, exemplified by compound **10** (Table 1), which was originally discovered as a CDK2 inhibitor in vitro,[36] produced cell cycle profiles that were inconsistent with CDK2 inhibition as a primary mechanism of action. Compound **10** also displayed potent cytotoxicity against a number of tumor cell lines (e.g., HT-29 colorectal cell line 96 h MTT IC_{50} = 128 nM), which did not apparently correlate with known biochemical kinase inhibition potency; compound **10** inhibited CDKs at K_i > 250 nM in biochemical kinase assays (Table 2). We therefore suspected that a compound subset mechanistically related to **10** may have relevant cellular antiproliferative targets other than CDKs.

Clinical CDK inhibitor compounds such as, 2-(2-chlorophenyl)-5,7-dihydroxy-8-[(3*S*,4*R*)-3-hydroxy-1-methyl-4-piperidinyl]-4*H*-1-benzopyran-4-one (flavopiridol, alvocidib)[43] and (2*R*)-2-[[9-(1-methylethyl)-6-[(phenylmethyl)amino]-9*H*-purin-2-yl]amino]-1-butanol (roscovitine, seliciclib)[44] are thought to act through inhibition of CDK2, CDK7, and CDK9.[45] These CDKs activate RNAPII through phosphorylation

of its C-terminal domain, and inhibition of this process results in rapid down-regulation of proteins with short-lived transcripts. For example, it had previously been observed that treatment of cells with roscovitine led to increased levels of the tumor suppressor protein p53, due to inhibition of transcription and down-regulation of its negative regulator, the ubiquitin ligase Mdm2.[46,47] We therefore evaluated elevated p53 levels as a marker of CDK inhibition, using an automated microscopy assay, which employed an anti-p53 antibody to assess the number of cells expressing a threshold level of p53. Analysis of our 2,4-bis(aryl)pyrimidin-2-amines revealed a group of compounds that at antiproliferative concentrations induced elevated p53 levels in several tumor cell lines. This group was typified by compound **9**, a known potent CDK2−CDK9 inhibitor, whose antiproliferative mechanism in cancer cells we have reported earlier.[36] As expected, this compound induced high p53 levels in cancer cell lines within 7 h at concentrations as low as 150 nM (Figure 1a). By contrast, a proportion of compounds in the collection (representative compounds **12−15** and **17−20** shown in Figure 1) did not induce an appreciable increase in p53 protein levels within the same time frame at submicromolar concentrations, despite their evident efficacy in antiproliferative assays (Table 2).

Table 2. Summary of Kinase Inhibition and Antiproliferative Activity of Test Compounds

| | CDK inhibition, K_i (nM)[a] | | | | | 96 h MTT, IC$_{50}$ (nM)[b] | | pS10H3, IC$_{50}$ (μM)[c] | aurora inhibition, K_i (nM)[a] | |
| | | | | | | | | A549 | | |
compd	CDK1	CDK2	CDK4	CDK7	CDK9	A2780	MiaPaCa-2		A	B
9	80	2	53	70	4	48	139		73	57
10	2520	251	1503	4012	575	157	177	2.60	6.9	15
11	909	286	840	4240	348	147	235	1.76	18	33
12	769	168	807	2556	337	584	1228	0.94	31	NT
13	706	239	666	243	11	10	22	0.13	0.4	2.0
14	367	256	955	370	6	24	62	0.28	1.0	3.0
15	1224	463	>10000	1395	564	389	994	1.88	3.0	6.0
16	240	32	38	171	9	81	230	0.76	5.0	4.0
17	>10000	1039	2170	>10000	>10000	332	871	0.86	4.0	9.0
18	>10000	390	1090	>10000	480	170	278	0.48	8.0	9.2
19	3925	156	943	>10000	2605	144	273	3.70	19	9.4
20	>10000	151	196	>10000	559	81	173	0.57	14	6.0
21	>10000	522	1248	2149	264	240	493	0.59	7.6	3.8
22	851	297	22	1080	448	221	622	NT	12	9.7
23	1894	432	929	2804	1153	303	604	0.36	8.2	13
24	>10000	3967	>10000	>10000	1472	298	608	1.11	9.2	18

[a] Calculated K_i values are averages from at least two independent determinations. [b] Concentration to inhibit 50% cell growth. Values are averages from at least two independent dose−response curves. [c] Concentration for half-maximal inhibition of pS10H3 immunofluorescence in A549 cells. Values are normalized for MPM2 staining (see text).
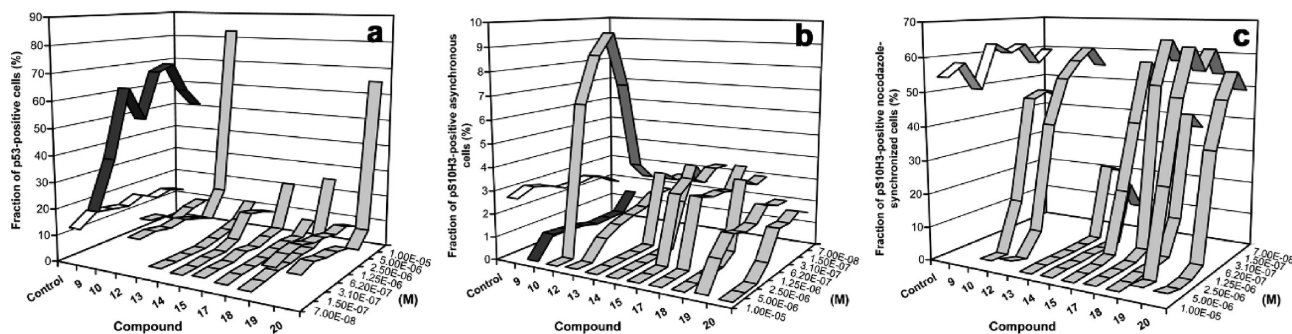

Figure 1. Cell-based screening cascade: increase in p53 protein expression detected by anti-p53 antibody in MCF7 cells (a); levels of pS10H3 in unsynchronized (b) or nocodazole-synchronized U2OS cells (c). Treatment with test compounds (or diluent only, control) was for 7 h.

Histone H3 serine-10 phosphorylation (pS10H3) is commonly used as a marker of mitotic index (percentage of cells in mitosis),[48] and we devised another automated microscopy assay based on pS10H3 immunofluorescence.[49] CDK inhibitors typified by compound **9**, which potently induced p53, blocked cells in G1/S, thus preventing entry into G2/M.[36] As expected, **9** reduced pS10H3 in asynchronous U2OS cells after 7 h treatment at concentrations as low as 150 nM (Figure 1b). Compounds that did not induce p53, on the other hand, either had little effect (e.g., **12**, **19**, and **20**) or caused pS10H3 elevation (e.g., **13**−**15**, **17**, **18**, and most pronouncedly **10**) at low concentrations at the 7 h time point, whereas all of them suppressed cellular pS10H3 at high concentration (Figure 1b). Because changes in pS10H3 may result as a consequence of the effect on the kinase catalyzing the phosphorylation and/or cell cycle arrest at different phases, we examined pS10H3 levels in cells presynchronized in mitosis with the mitotic spindle disruptor nocodazole (Figure 1c).[50] Control cells retained a high proportion of pS10H3-positive cells after 2 h, indicating effective mitotic synchronization, whereas those treated with compounds that did not induce p53 had lost pS10H3 staining at submicromolar concentrations. Normalization of the data against cellular immunofluorescence staining with the MPM2 antibody, which recognizes a large range of phosphoepitopes specific for mitotic proteins,[51] permitted us to

calculate half-maximal inhibition (IC$_{50}$) values for the loss of pS10H3 in the mitotic cell population (Table 2).

We next conducted cell cycle analyses to shed light on the possible cellular mode of action of the compounds that did not induce p53. Treatment of asynchronous A549 cells with, for example, compound **10** resulted in accumulation of cells in G2/M (cyclin B-positive with 4 n DNA content) at 7 h, while by 24 h most of the cells treated with 0.5 μM compound **10** were in G1 (2 n DNA, cyclin B-negative). After 24 h of treatment with 2.0 μM compound **10**, cyclin B1-negative G1 cells with 2 n and 4 n DNA were observed, indicating that many of the cells had failed to complete cytokinesis and were tetraploid (Figure 2a). The mitotic cells had multiple acentrosomal microtubule-nucleating centers, misaligned chromosomes, and shortened spindles with minispindle-like structures forming around or toward misaligned groups of chromosomes (Figure 2b, parts iii and iv). The presence of monopolar spindle structures was also observed in some cells. Similarly, in the same assay, compound **18** greatly increased the number of tetraploid cells in G1 (cyclin B1-negative with 4 n DNA content), and by 24 h the number of cells with >4 n DNA content was also increased (Figure 2a). Although there were fewer mitotic cells after treatment with **18**, the remaining mitotic cells showed phenotypes similar to those seen after treatment with **10** (Figure 2b, parts v and vi).
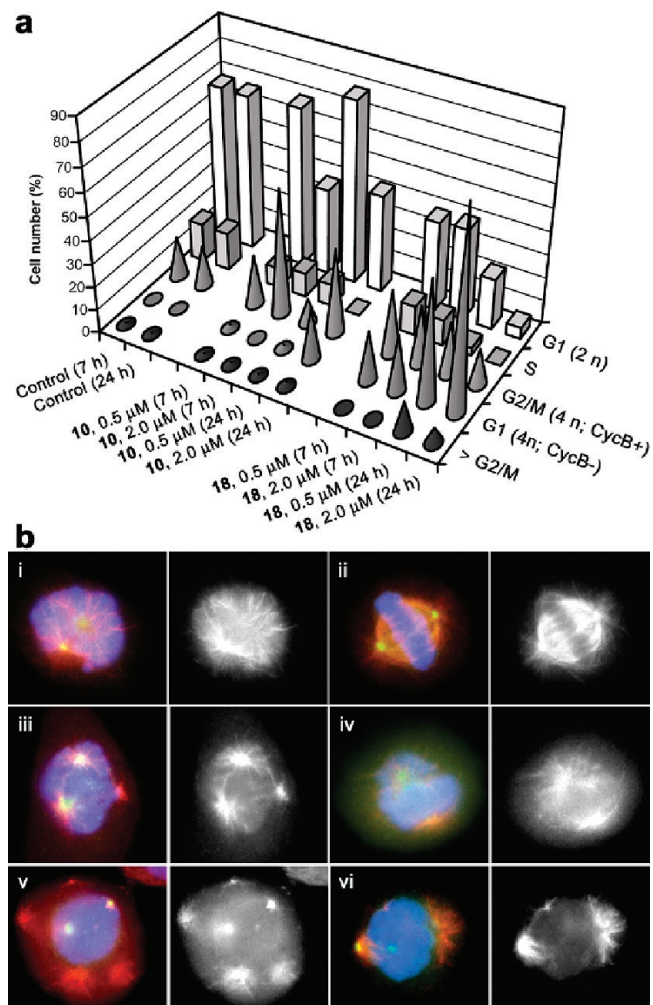
Figure 2. Effect of cell treatment with test compounds on mitotic index: (a) flow cytometric analysis of cell cycle progression of A549 cells after staining for DNA and cyclin B1 content; (b) fluorescence microscopy of A549 mitotic cells. DNA (blue), α-tubulin (red), and centrosomal γ-tubulin (green) with α-tubulin alone shown in right-hand panels (black and white). Control untreated cells are in pro-metaphase (i) and metaphase (ii). Cells were treated with 0.5 μM **10** for 8 h (iii, iv), and cells were treated with 0.5 μM **18** for 8 h (v, vi).

Compounds mechanistically related to **10** and **18** thus appeared to override mitotic checkpoints so that cells failed correctly to segregate their chromosomes and after defective cytokinesis exited mitosis in a polyploid state. Suppression of pS10H3 in the mitotic cell population (MPM-2 positive) by these compounds was likely to be due to cellular inhibition of the kinases responsible for the phosphorylation of serine-10 of histone H3, such as aurora B.[52,53] Together, these findings pointed toward aurora kinases as the likely targets. Although the observed cellular phenotypes of mitotic aberrations and polyploidy are now familiar from numerous reports on aurora kinase inhibitors (reviewed in refs 4, 24, and 54), at the time of carrying out the work described here such compounds had not as yet been reported, but the phenotypes were reminiscent of our earlier observations in connection with the discovery and characterization of *Drosophila* aurora kinases.[55−57] Subsequent testing in biochemical kinase assays confirmed that compounds **10−24** were indeed potent inhibitors of aurora A and B kinases (Table 2).

SAR Analysis. CDK and aurora kinase inhibitory activities for the test compounds (Table 1), as well as cellular antiproliferative activities, are summarized in Table 2. In contrast to the 3-nitroaniline **9**, which we used as a structurally related prototype CDK2−CDK9 inhibitor in the present study and which was > 14-fold selective for CDK2 and CDK9 over aurora kinases, the 4-(dimethylamino)aniline **10** was > 16-fold selective for aurora kinases over CDK2 and CDK9. The closely related 4-methylamino and 4-amino derivatives **11** and **12** were somewhat less potent and less selective aurora inhibitors, suggesting that steric bulk at the aniline para position was a determinant for both aurora potency and selectivity. However, physicochemical and stereoelectronic properties may also contribute to aurora selectivity, especially by influencing charge distribution of the aniline NH bond to strengthen the H-bond formed with the Leu83 carbonyl group. The most potent aurora kinase inhibitors, with low single-digit nanomolar or subnanomolar K_i values, were the 3,4,5-trimethoxyanilines **13−15**. Here the presence of the thiazole C2-ethylamino group in **15** was clearly beneficial in terms of aurora selectivity, especially with respect to CDK9, compared to **13** and **14**, which contained the somewhat smaller thiazole C2-methyl and -methylamino groups and were poorly selective with respect to CDK9. Compound **16**, on the other hand, which also contained the thiazole C2-ethylamino group but a 4-(acet-amidomethyl)aniline instead of the trimethoxyaniline, while potent against aurora kinases, was poorly selective, especially over CDK2, CDK4, and CDK9. Like the 4-(di-methylamino)aniline **10**, the 4-morpholinoanilines **17−20** were also potent and selective aurora kinase inhibitors and there was no clear influence of the thiazole C2 substituent on kinase potency and selectivity or cellular activity. The 4-(4-acetylpiperazin-1-yl)anilines **21−23** presented a similar picture. Finally, the 4-(4-(methylsulfonyl)piperazin-1-yl)aniline **24** was another potent and selective aurora kinase inhibitor.

We had previously solved X-ray crystal structures of a number of 4-(thiazol-5-yl)pyrimidin-2-amines in complex with CDK2, and the binding mode and SARs with respect to CDKs are understood to some extent.[34−38] We have also now determined the structure of the complex between CDK2/cyclin A and compound **18** (Figure 3a,b,d). In this complex, the ligand was observed to recognize the ATP-binding pocket through the characteristic hydrogen-bonding network involving the interdomain connecting loop (hinge region, residues Phe80−Gln85), especially Leu83 (Ala213 in aurora A), whose backbone amide NH and carbonyl functions formed hydrogen bonds with the pyrimidine N1 and C2-NH groups of the ligand (Figure 3b). The thiazole ring occupied a position near the gatekeeper residue and extended into the ribose pocket, resulting in hydrophobic interaction between the thiazole C4-methyl group and the phenyl ring of the gatekeeper residue (Phe[80] in CDK2, Leu[210] and Leu[170] in aurora A and B, respectively). The aniline moiety extended toward the solvent-accessible exterior of the ATP-binding pocket (Figure 3d). We had previously established that small polar substituents at the meta-position of the aniline, such as the nitro group in compound **9**, generally enhanced CDK inhibition, in particular that of CDK2.[36] A hypothesis for the aurora kinase potency and selectivity of **18** and other para-substituted aniline analogues was generated by comparison of the experimental CDK2 complex structure of **18** with the modeled binding pose of this compound in the ATP-binding pocket of aurora A kinase (Figure 3c,e). Overall, the binding poses were similar, but a distinctive feature of aurora A is the insertion of a glycine residue (Gly216) in the hinge region.
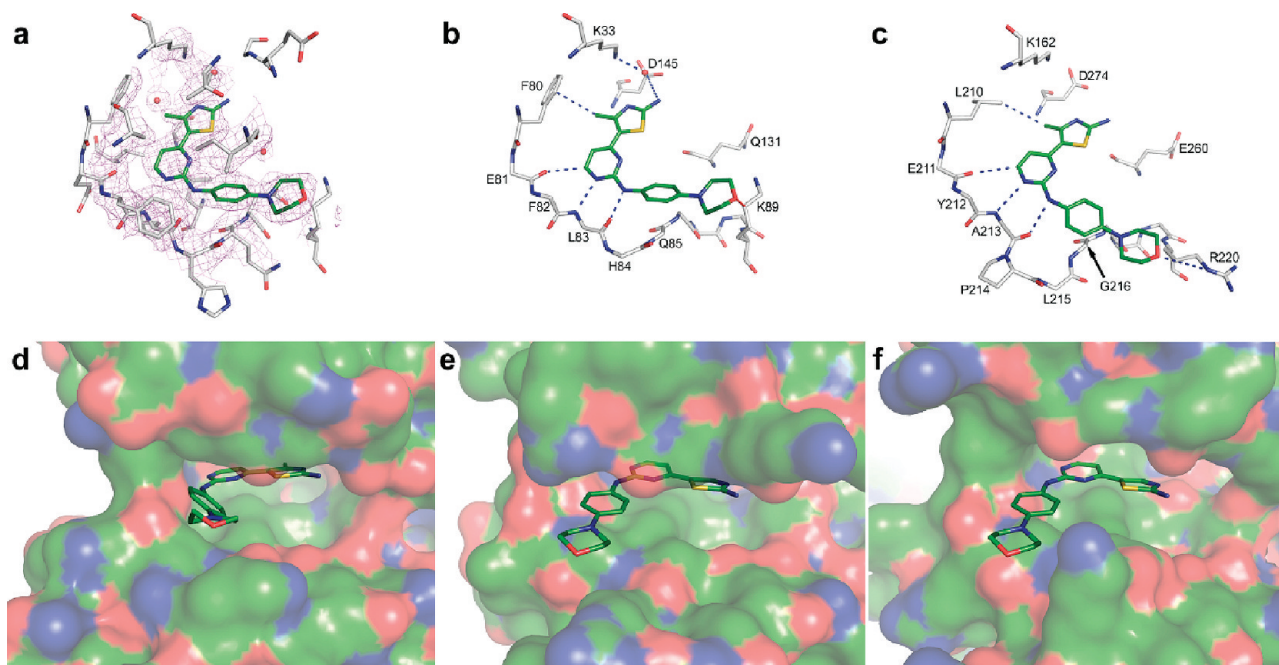
Figure 3. CDK2 and aurora kinase binding modes of compound **18** (green CPK stick models). (a) Electron density (contoured at 1σ) within 5 Å of the ligand in the X-ray crystal structure (PDB code 2UUE) of **18** in complex with CDK2/cyclin A (only residues in close contact with ligand are shown as gray CPK sticks). Binding pose of compound **18** in the ATP-binding cleft of CDK2 (b) and modeled pose in aurora A kinase (c) (based on ADP/Mg complex PDB code 1OL7[64]). Favorable contacts (hydrophobic and H-bonds) are indicated with broken blue lines. An unfavorable interaction between the morpholine O of **18** with $C^\gamma H_2$ of K89 in CDK2 is shown as a broken red line. Inhibitor poses with protein surfaces (CPK coloring) are shown for CDK2 (d), aurora A (e), and aurora B (f) (based on hesperadin complex PDB code 2BFY[72]). The residues in proximity to **18** in the ATP-binding pocket of the modeled complex with aurora A are identical in aurora B (Y212 is F172 and L215 is R175 in aurora B, but the side chains project away from the ligand) with the exception of R220, which is K180 in aurora B.

This extra residue, together with proline-214, creates a bulge, giving a more open conformation of the interdomain connecting loop. Gly216 in aurora A aligns with Gln85 in CDK2, and the former provides a greater volume to accommodate aniline ring substitutions. This extra space in aurora A (Figure 3e), as well as in aurora B, which displays a similar configuration as aurora A (Figure 3f), can thus accommodate anilines para-substituted with comparatively large groups better than CDK2 (Figure 3d). Docking experiments additionally suggested more favorable contacts of, for example, the morpholine ring with Arg220 in aurora A than the corresponding residue (Lys89) in CDK2, with the ring oxygen directly hydrogen-bonding to the guanidine group in the arginine side chain (Figure 3b,c). In both CDK2 and aurora A binding modes the thiazole C2-NH_2 group of **18** was in proximity to Lys33 and Asp145 (Lys 162 and Asp274 in aurora A) for potential polar interactions. This may explain the fact that no clear SARs were observed as far as the thiazole C2 substituents are concerned.

Kinase Selectivity. As can be seen from Table 1, the most aurora-selective compounds **17**, **18**, and **24** inhibited aurora A and B kinases about 50-fold more potently than any of the CDKs assayed. Compound **18** was also assessed against other kinases (Table 3). It was not active against serine/threonine protein kinases A, B, and C (PKA, Akt/PKB, PKC) and had no effect on glycogen synthase kinases-3 (GSK-3α and GSK-3β), extracellular signal-regulated kinase-2 (ERK2), calmodulin-dependent protein kinase II (CaMKII), casein kinase 2 (CK2), polo-like kinase 1 (Plk1), and stress-activated protein kinase 2A (SAPK2A). However, it inhibited two tyrosine kinases, FMS-like tyrosine kinase 3

Table 3. In Vitro Kinase Selectivity of Compound **18**

protein kinase	$K_i \pm SD$ (μM)
aurora A	0.008 ± 0.004
aurora B	0.009 ± 0.005
CDK1/cyclin B	> 10
CDK2/cyclin E	0.39 ± 0.19
CDK4/cyclin D	1.09 ± 0.32
CDK7/cyclin H	> 10
CDK9/cyclin T	0.480 ± 0.202
Abl	> 10
Akt/PKB	> 10
CaMKII	> 10
CKII	> 10
ERK2	> 10
Flt-3	0.044 ± 0.067
GSK-3α	> 10
GSK-3β	> 10
PKA	> 10
PKC	> 10
SAPK2A (p38)	> 10
Plk1	> 10
p70 S6	0.54 ± 0.29
Src	0.82 ± 0.33
Lck	2.80 ± 0.71
VEGFR2	0.044 ± 0.020

(FLT3) and vascular endothelial growth factor receptor 2 kinase (VEGFR2), with a K_i value of ~44 nM in both cases. Potent inhibition of FLT3, which is closely related to VEGFR2, has previously been reported for aurora kinase inhibitors structurally unrelated to our compounds.[54] Compound **18** also showed low micromolar activity against 70 kDa ribosomal protein S6 kinase (p70S6K), Src, and lymphocyte-specific protein tyrosine kinase (Lck). Finally, compound **18**

Table 4. Antiproliferative Activity against Cancer Cell Lines of Compounds **10** and **18**

| human cell line | | 96-h MTT, IC$_{50}$ ± SD (μM) | |
origin	designation	**10**	**18**
breast	MCF7	0.960 ± 0.321	0.599 ± 0.161
cervix	HeLa	0.190 ± 0.042	0.590 ± 0.176
colon	Colo205	0.084 ± 0.004	0.241 ± 0.034
	HCT-116	0.133 ± 0.051	0.340 ± 0.156
	HT29	0.128 ± 0.049	0.725 ± 0.305
leukemia	K562	0.04 ± 0.001	1.375 ± 0.414
	CCRF-CEM	0.17 ± 0.007	0.471 ± 0.055
	MV4−11	0.11 ± 0.008	0.034 ± 0.011
	HL60	0.128 ± 0.007	0.372 ± 0.043
lung	NCI-H460	0.18 ± 0.007	0.681 ± 0.228
ovarian carcinoma	A2780	0.112 ± 0.039	0.151 ± 0.028
pancreatic carcinoma	BxPC3	0.093 ± 0.031	1.626 ± 0.817
	HuPT4	0.156 ± 0.064	0.775 ± 0.450
	Mia-Paca-2	0.081 ± 0.120	0.308 ± 0.058
bone	Saos-2	0.320 ± 0.100	0.110 ± 0.098
uterine	Messa	0.110 ± 0.046	0.090 ± 0.046
median		0.128	0.422
mean		0.187	0.537

was also screened against a more extensive panel of serine/threonine protein kinases, and the results are shown in Supporting Information Figure 1. A number of these kinases were inhibited, most of which at concentrations several orders of magnitude higher than those resulting in aurora A and B inhibition. Exceptions were SGK (serum and glucocorticoid-inducible kinase) and CK (casein kinase) 1, against which more potent inhibition was observed.

Biopharmaceutical Properties and Pharmacokinetics. Compounds **10** and **18** were also assessed for their in vitro ADME properties (Table 4 and Table 5). Compound **18** was found to be somewhat more lipophilic than **10**, and although the intrinsic aqueous solubility of both compounds appeared low, solubility at lower pH was enhanced because of the comparatively low pK_a values of both compounds.[58] For the prediction of intestinal absorption, determination of the permeation rate of compounds through a Caco-2 cell monolayer was used. It has been shown that drugs with an apparent permeability coefficient (P_{app}) of $> 33 \times 10^{-6}$ cm/s in the Caco-2 permeability assay were completely absorbed by the human body.[59] Both **10** and **18** were found to be highly permeable with $P_{app} > 47 \times 10^{-6}$ cm/s (Table 5). We used compound incubations with liver microsome fractions for initial assessment of metabolism.[60] Compound **18** exhibited better metabolic stability than **10**, with a 7-fold longer half-life and lower clearance. A human hepatocyte metabolism assay was subsequently used to show that rapid metabolism in the case of compound **10** was due to formation of the desmethylated species corresponding to the synthetic compound **11** (Table 1). Finally, plasma protein binding was significantly lower for compound **18** than for compound **10**.

From these results compound **18** was predicted to possess better intestinal absorption and pharmacokinetic (PK) properties compared to **10**, and an initial rat PK analysis was conducted. Profiles were determined following a single intravenous bolus dose at 5 mg/kg and an oral dose at 10 mg/kg. PK parameters are summarized in Table 6. At an oral dose of 10 mg/kg, compound **18** showed a 4-fold higher maximum plasma concentration (C_{max}) and a 2-fold increase in the area under the concentration−time curve (AUC) compared with those of **10**. At 38%, the oral bioavailability of **18** was > 5-fold higher than that of **10**. In an escalating oral dose

Table 5. Biopharmaceutical and in Vitro Pharmacokinetic Property Comparison of Compounds **10** and **18**

| parameter | | compd | |
		10	**18**
partition coefficient	$\log D_{7.4}$ [a]	1.33	2.74
dissociation constant	pK_a [b]	5.5, 2.8	4.4, 3.1
aqueous solubility[c]	μM	20.0	10.5
intestinal permeability	P_{app} (10^{-6} cm/s) [d]	49.19	47.04
microsomal stability[e]	CL$_{int}$ ((mL/min)/mg)	296.13	42.29
	$t_{1/2}$ (min)	4.7	32.8
plasma protein binding[f]	fraction bound (%)	96	93

[a] Partitioning between octanol and aqueous buffer using the shake-flask method. [b] Determined using a pH-metric method. [c] By turbidimetry. [d] Apparent permeability coefficient measured using a Caco-2 cell layer assay. [e] Measured by disappearance of parent compound (LC−MS) from a preparation of rat liver microsomes. [f] Rat plasma protein binding using an equilibrium dialysis assay.

Table 6. Rat Pharmacokinetic Comparison of Orally Administered Aurora Kinase Inhibitor Compounds **10** and **18**[a]

| parameter | | compd | |
		10	**18**
exposure	C_{max} (μM)	0.9	3.9
	AUC$_{0-24h}$ (h·μM)	6.9	13.6
elimination	$t_{1/2}$ (h)	4.4	3.0
clearance	CL ((L/h)/kg)	4.2	2.0
volume of distribution	V$_z$-F (L/kg)	26.8	8.5
oral bioavailability	F (%)	7	38

[a] Dosed at 10 (mg/kg)/dose.

study of **18** in mice, it was found that bioavailability was higher (up to 61%) and the exposure increased in a linear fashion as a function of dose up to 100 mg/kg (not shown). Considering the in vitro antiproliferative potency of **18** (Table 4), these results suggested that potentially bioactive in vivo concentrations should be able to be achieved readily.

Metabolic stability toward polymorphic cytochrome P450 (CYP) enzymes of **18** was assessed using the recombinant human isoforms CYP1A, CYP2C9, CYP2C19, CYP2D6, and CYP3A4. **18b** was not a significant substrate for metabolism at 5 μM, and an in vitro elimination half-life could only be determined with CYP1A2 ($\sim$72 min). Furthermore, **18** did not induce CYP3A in human hepatocytes, although at 1 μM some induction of CYP1A was observed. Compound **18** was also assessed in terms of potential cardiotoxicity, but no concentration-dependent hERG (human ether-a-go-go-related gene) inhibition was recorded at concentrations up to 50 μM.

Cellular Mode of Action. On the basis of its in vitro potency, selectivity, and favorable biopharmaceutical properties, the cellular mode of action of **18** was evaluated. The compound was initially screened against a panel of human leukemia and solid tumor cell lines using an MTT antiproliferative assay,[61] and results are summarized in Table 4. IC$_{50}$ values were in the mid-nanomolar to high nanomolar range throughout, which suggests that compound **18** may have broad-spectrum antitumor activity. Of the leukemia cancer cell lines tested, compound **18** was particularly cytotoxic against the acute myelogenous leukemia cell line MV4-11. Apart from aurora kinase inhibition, this could be a consequence of additional FLT3 inhibition by **18**, since this cell line expresses a constitutively active mutant FLT3 receptor protein.[62]

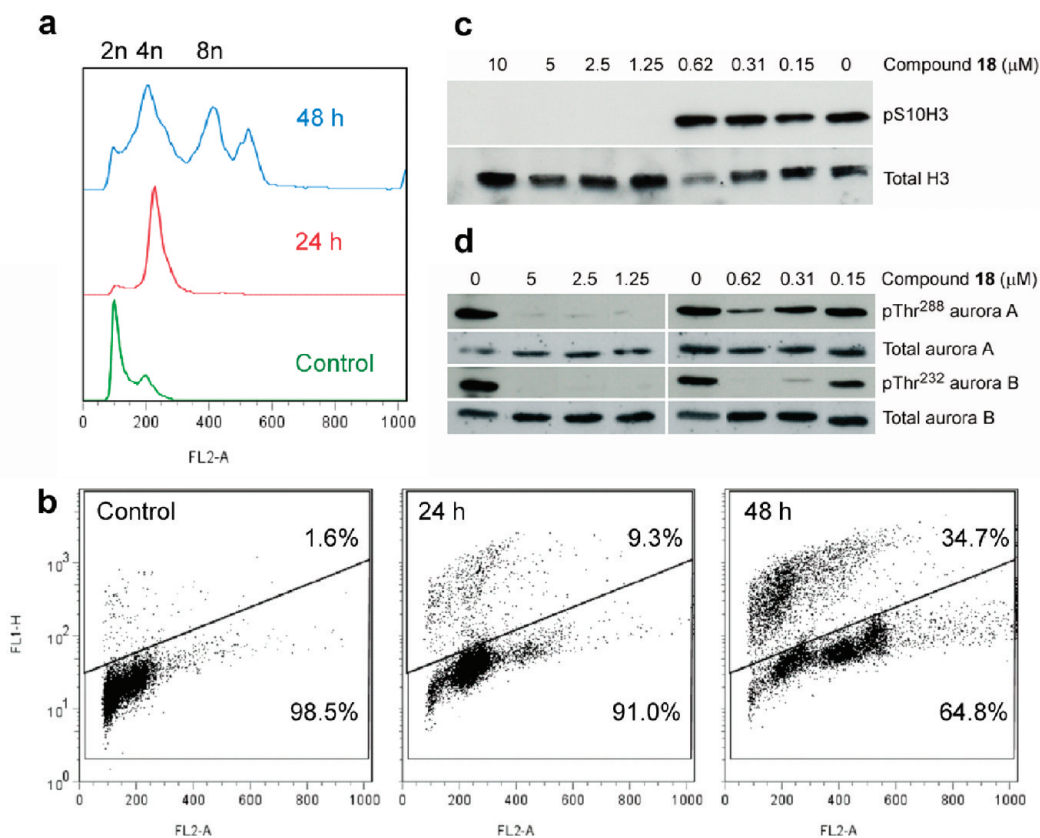In order to investigate the observed increase in polyploidy, the DNA content of SW-680 cells (colon carcinoma), treated

Figure 4. Cellular effects of compound **18**. SW-620 cells were treated with 1 μM compound **18** for 24 and 48 h. Cell cycle profiles (a) show an increase in polyploidy with cells moving into a > 4 n DNA population at 48 h treatment (*Y*-axis, percentage of maximum signal; *X*-axis, DNA content by PI staining). Polyploidy is accompanied by apoptosis as measured by TUNEL staining (*Y*-axis) of cells (b). Western blot of phosphorylated histone H3 Ser10 and total histone H3 of HeLa cells 7 h after treatment (c). Western blot showing loss of aurora A phosphothreonine-288 and aurora B phosphothreonine-232 after 1 h of treatment of A549 cells blocked in mitosis in the presence of nocodazole and the proteasome inhibitor MG132 (d).

with 1 μM compound **18**, was followed for 48 h (Figure 4a). SW-680 cells became increasingly polyploid, developing 4 n and > 4 n DNA peaks; polyploidy was accompanied by apoptosis, as measured by TUNEL staining (Figure 4b). The effect on cellular biomarkers of aurora kinase inhibition was studied in different cell lines. Western blotting of HeLa cell lysates shown in Figure 4c revealed that treatment with 1.25 μM **18** for 7 h resulted in complete inhibition of histone H3 phosphorylation. There appeared to be genuine inhibition of histone H3 staining rather than a decrease in the percentage of mitotic cells, since fluorescence staining of mitotic cells with the same anti-pS10H3 antibody showed that mitotic cells with condensed DNA were present, but after treatment with 1.0 μM **18** the pS10H3 staining was lost (not shown). Western blotting of lysates from A549 cells trapped in mitosis by treatment with nocodazole and the proteasome inhibitor MG132, which prevents mitotic exit,[63] showed that compound **18** inhibited autophosphorylation of both aurora A[64,65] and B[66] at antiproliferative concentrations in cells (Figure 4d). It can therefore be concluded that the major cause of cellular aberration and death induced by compound **18** is likely to be inhibition of aurora kinases.

In Vivo Antitumor Activity. Compound **18** was first evaluated in the P388/D1 murine leukemia model.[67] Animals implanted intraperitoneally with P388/0 cells were treated with **18**, and the antitumor activity was measured as an increase in lifespan of the treated animals versus the vehicle control group. As shown in Supporting Information Figure 2a, compared to controls, oral dosing at 45 and 67 mg/kg twice daily on days 1−5 and 7−9 resulted in a significant increase in lifespan (ILS) of 172% and 183%, respectively. In vivo efficacy of **18** was also evaluated in several human tumor xenograft models and demonstrated substantial inhibition of tumor growth.[68,69] For example, animals bearing subcutaneous NCI-H460 xenografts were given **18** orally for 5 days once tumors had been established (Supporting Information Figure 2b). When calculated to 4-fold tumor volume increase compared to vehicle controls, oral administration of **18** at dose levels of 75 and 100 mg/kg q.d. caused tumor growth delays of 2.3 and 5.8 days, which translated into specific growth delays of 0.32 and 0.81, respectively. The mean relative tumor volumes of mice receiving **18** at both dose levels were less than those of vehicle-treated mice for the duration of the study period. At 100 mg/kg po q.d., the reduction in growth (ratio of mean relative tumor volumes in treated and control groups, T/C) was statistically significant on days 6 and 9 (40% T/C, $P < 0.05$ and 19% T/C, $P < 0.001$). Some animals treated at 100 mg/kg q.d. with **18** suffered weight loss by day 8; however, their weights had returned to normal by day 13. No signs of toxicity or body weight loss were observed in the 75 mg/kg q.d. **18** treatment group.

Conclusions

We have described the discovery of a series of substituted 4-(4-methylthiazol-5-yl)-*N*-phenylpyrimidin-2-amines **10−24**, which are potent aurora kinase inhibitors, using cell-based

screening strategies in which cell cycle effects and phenotypes were assessed. SARs with respect to CDKs and aurora kinases were rationalized, and lead compound **18** was examined in more detail regarding cellular mode of action. Antiproliferative activity was associated with biological changes consistent with aurora A and B modulation, i.e., inhibition of aurora autophosphorylation, reduction of histone H3 phosphorylation, and polyploidy, followed by cell death, resulting from a failure in cytokinesis. ADME assessment of compound **18** was carried out, and initial signs of efficacy by the oral administration route in animal tumor models were obtained. Preliminary data on the in vivo mode of action of compound **18** (CYC116), which is currently undergoing clinical trials in cancer patients, have been presented.[68,69]

Experimental Methods

Synthesis and Compound Characterization. Melting points were determined with a Leica Testo-720 electrothermometer instrument and are uncorrected. NMR spectra were obtained using a Varian INOVA-500 instrument. Chemical shifts are reported in parts per million (ppm) relative to the internal tetramethylsilane (Me_4Si) standard. Fast atom bombardment (FAB) high-resolution mass spectra were recorded on a Kratos MS50TC instrument. Silica gel (EM Kieselgel 60, 0.040−0.063 mm, Merck) or ISOLUTE prepacked columns (Argonaut) were used for flash chromatography.[70] Target compounds for which elemental microanalysis was not obtained or for which analytical results obtained were not within 0.4% of calculated values were further analyzed using two different RP-HPLC systems: linear gradient elution using H_2O/MeCN (containing 0.1% CF_3COOH) or H_2O/MeOH (containing 0.1% CF_3COOH). In both cases a flow rate of 1 mL/min and a gradient elution time of 20 min, using a Vydac 218TP54 (250 mm × 4.6 mm) column and a diode array detector, were used. Compound purities by RP-HPLC (integration of chromatograms at $\lambda = 254$ nm) were ≥95% throughout.

General Procedure for the Preparation of *N*-Phenyl-4-(thiazol-5-yl)pyrimidin-2-amines.[36] A mixture of the appropriate 3-dimethylamino-1-thiazol-5-ylpropenone **4** (1 equiv), 1-phenylguanidine hydrochloride or nitrate **8** (2 equiv), and NaOH (1 equiv) in 2-methoxyethanol (0.2 mL/mmol) was heated at 125 °C for 22 h under N_2. After the mixture was cooled, the solvent was evaporated and the residue was purified by flash chromatography using appropriate mixtures of EtOAc and hexane as the eluant. The products **9**−**24** were further purified by crystallization from EtOAc−MeOH mixtures.

N[1]-[4-(2,4-Dimethylthiazol-5-yl)-pyrimidin-2-yl]-*N*′,*N*′-dimethylbenzene-1,4-diamine (10). 10 was obtained by condensation between enaminone **4a** and phenylguanidine **8b**. Yellow crystals (72%); mp 236−238 °C. RP-HPLC: t_R = 11.2 min (0−60% MeCN, purity 97%). ^{1}H NMR (DMSO-d_6): δ 2.60 (s, 3H, CH_3), 2.62 (s, 3H, CH_3), 2.82 (s, 6H, CH_3), 6.70 (d, 1H, J = 8.8 Hz, Ph-H), 6.94 (d, 1H, J = 5.3 Hz, pyrimidinyl-H), 7.53 (d, 1H, J = 9.0 Hz, Ph-H), 8.40 (d, 1H, J = 5.3 Hz, pyrimidinyl-H), 9.27 (s, 1H, NH). ^{13}C NMR (CDCl$_3$): δ 16.47, 17.71, 39.52, 106.51, 111.77, 120.38, 127.53, 129.73, 145.76, 150.50, 156.83, 157.40, 158.75, 165.03. MS (ESI[+]): *m/z* 326.20 [M + H][+]. Anal. (C$_{17}$H$_{19}$N$_5$S) C, H, N.

4-Methyl-5-(2-(4-morpholinophenylamino)pyrimidin-4-yl)thiazol-2-amine (18). 18 was obtained by condensation between enaminone **4b** and phenylguanidine **8g**. Yellow solid (77%); mp 300−304 °C. RP-HPLC: t_R = 8.28 min (10−70% MeCN, purity 100%). ^{1}H NMR (DMSO-d_6): δ 2.42 (s, 3H, CH_3), 3.02 (m, 4H, CH_2), 3.73 (m, 4H, CH_2), 6.80 (d, 1H, J = 5.0 Hz, Py-H), 6.86 (d, 2H, J = 9.5 Hz, Ph-H), 7.45 (bs, 2H, NH$_2$), 7.61 (d, 2H, J = 9.5 Hz, Ph-H), 8.26 (d, 1H, J = 5.0 Hz, Py-H), 9.17 (bs, 1H, NH). ^{13}C NMR (DMSO-d_6): δ 19.11, 50.03, 66.89, 106.95, 116.24, 118.91, 120.72, 133.84, 146.63,

152.40, 156.26, 159.33, 160.29, 169.41. MS (ESI[+]): *m/z* 368.98 [M + H][+]. Anal. (C$_{18}$H$_{20}$N$_6$OS) C, H, N.

Kinase Assays. These were carried out as described previously.[36] IC$_{50}$ values were determined using XLfit software (IDBS). Apparent inhibition constants (K_i) were calculated from IC$_{50}$ values and the appropriate K_m (ATP) values for each kinase using the method of Cheng and Prussoff.[71] Recombinant human aurora A and B kinases were purchased from Upstate Discovery. Aurora A kinase assays were performed using a 25 μL reaction volume (25 mM β-glycerophosphate, 20 mM Tris/HCl, pH 7.5, 5 mM EGTA, 1 mM DTT, 1 mM Na$_3$VO$_4$, 10 μg of kemptide (peptide substrate)), and recombinant aurora A kinase was diluted in 20 mM Tris/HCl, pH 8, containing 0.5 mg/mL BSA, 2.5% glycerol, and 0.006% Brij-35. Reactions were started by the addition of 5 μL Mg/ATP mix (15 mM MgCl$_2$, 100 μM ATP, with 18.5 kBq γ-^{32}P-ATP per well) and incubated at 30 °C for 30 min before terminating by the addition of 25 μL of 75 mM H$_3$PO$_4$. Aurora B kinase assays were performed as for aurora A except that prior to use, aurora B was activated in a separate reaction at 30 °C for 60 min with inner centromeres protein (INCENP, Upstate).[72]

p53 Stabilization Assay. Cells were plated at 10[4] cells per well and incubated for 18 h at 37 °C. Test compounds were added, and the cells were incubated for the appropriate time before a 3 min fixation in cold (−20 °C) 50:50 v/v MeOH/Me$_2$CO. The fixed cells were dried briefly and then washed with PBST (PBS, 0.1% Triton X-100) and incubated with primary antibody solution containing CM-1 rabbit antihuman p53 antiserum[73] diluted 1:1000. After incubation with a secondary antibody solution containing Alexa Fluor 488 goat antirabbit antibody (Molecular Probes, A11008) and Hoechst 33258 dye, the cells were washed and analyzed using a Cellomics ArrayScan II automated fluorescent microscopy system (Thermo Scientific) to detect nuclear fluorescent staining. Data for 2000 cells per well were collected, and the Cellomics mitotic index algorithm was used to calculate percentage of cell nuclei stained with p53-specific antibody versus total cell nuclei stained with Hoechst 33258 dye.

Mitotic Index Assay. This was carried out with an automated fluorescence microscopy 96-well plate assay using a Cellomics ArrayScan II automated fluorescent microscopy system with the mitotic index HitKit protocol (Cellomics). Briefly, cells were plated at 10[4] cells per well and incubated for 18 h at 37 °C. Compounds were added and the cells incubated for the appropriate time before a 15 min fixation in 3.7% formaldehyde in PBS. The cells were permeabilized in PBS with 0.2% Triton X-100 for 15 min, washed, and incubated with primary antibody that specifically recognizes a mitotic epitope (rabbit anti-phosphoserine-10 histone H3, Upstate 06-570). After incubation with a secondary FITC-conjugated antirabbit antibody and Hoechst 33258 dye, the cells were washed and analyzed using the Cellomics ArrayScan II instrument to detect nuclear fluorescent staining. Data for 2000 cells per well were stored, and the Cellomics mitotic index algorithm was used to calculate mitotic index (percentage of cell nuclei stained with the mitosis-specific antibody versus total cell nuclei stained with Hoechst 33258).

Cell Cycle Analysis by Flow Cytometry. To synchronize cells in early S phase, they were subjected to double thymidine block. HeLa cells were seeded at 5 × 10^{5} cells per 10 cm dish and incubated for 16−18 h at 37 °C. Thymidine (2 mM) was added, and the cells were incubated for 18 h. The cells were released from the block by washing 3 times in 5 mL of PBS. Fresh medium was added, and the cells were incubated for 8 h. Then 2 mM thymidine was added again for a second period of 16 h. The cells were released again and fresh medium was added, together with test compound dilutions as appropriate.

To synchronize A549 cells in the M phase, they were incubated with 40 ng/mL nocodazole (Sigma) for 18 h. Where stated, cells were also treated with 50 μM MG132 proteasome inhibitor

(Sigma) for the final 2 h of the incubation. Rounded-up mitotic cells, detached from the plate by shaking off and repeated washing, were pelleted and washed in PBS to release from the nocodazole block. The cells were replated in fresh medium with test compound dilutions as appropriate.

Cell cycle analysis was performed on cells in conjunction with either TUNEL staining or cyclin B analysis. As such, all cells were harvested, washed in PBS, fixed with 0.5% PFA, and stored at −20 °C in 80% ethanol. Terminal deoxynucleotidyl transferase-mediated nick end labeling (TUNEL) assay (ApoDirect BD) was performed following manufacturer's instructions. Cyclin B analysis during flow cytometry used a 1:1000 dilution of cyclin B antibody (Abcam ab72-100) in 400 μL of 0.5% BSA PBS, with 1:400 FITC goat polyclonal to mouse secondary (Abcam, ab6785-1) followed by incubation with PI for DNA staining. The 20 000 single cell events per sample were analyzed using a BD FACSCalibur flow cytometer.

Western Blot Analysis of Histone H3 Phosphorylation. For detection of phosphorylated histone H3, HeLa cells were treated with compounds for 7 h. Then extracts were prepared by acid extraction. Briefly, the cells were scraped from the plates, pelleted, washed once in PBS, then resuspended in lysis buffer (10 mM Tris/HCl, pH 8.0, 1.5 mM MgCl$_2$, 10 mM KCl, 0.5 mM DTT) containing Roche complete protease inhibitor cocktail. HCl and H$_2$SO$_4$ were added to a final concentration of 0.2 M, and the lysates were incubated on ice for 1 h. Insoluble material was pelleted by centrifugation, and the acid-solubilized super-natant was added to 1 mL of Me$_2$CO and stored at −20 °C for 24 h. Precipitated protein was pelleted by centrifugation, air-dried briefly, and resuspended in SDS−PAGE loading buffer. The samples were separated on a 15% SDS−polyacrylamide gel and transferred to a nitrocellulose membrane by electroblotting. Phosphorylated histone H3 was detected on the membrane with rabbit anti-phosphohistone H3 antibody (Upstate 06-570), and total histone H3 was detected with mouse anti-histone H3 (Upstate 05-499), followed by appropriate secondary antibodies and chemiluminescent detection.

Western Blot Analysis of Aurora Autophosphorylation. Cell treatments and preparation of lysates were as above. Lysates were separated using 10% SDS−polyacrylamide gels and transferred to nitrocellulose filters. Primary antibodies used to detect proteins were rabbit anti-phospho-Thr232 aurora B (Cell Signaling Technology 3095), rabbit anti-phospho-Thr288-aurora A (Cell Signaling Technology 3091), rabbit anti-aurora B (Abcam ab2254), goat anti-aurora A/Ark1 (Santa Cruz sc-14318), mouse antihuman cyclin B1 (BD Pharmingen 554177), and mouse anti-β-actin clone AC-15 (Sigma A5441).

Immunofluorescence Microscopy. Cells were grown on sterile glass coverslips. After appropriate treatment, the culture medium was removed and the cells were fixed with MeOH at −20 °C for 3 min. The coverslips were allowed to air-dry, then washed with PBT (PBS containing 0.1% Triton) and incubated with primary antibodies diluted in blocking buffer (PBT containing 1% BSA). Primary antibodies used were rat anti-α-tubulin (Serotec YL1/2, diluted 1:500) and rabbit anti-γ-tubulin (Sigma DQ-19, diluted 1:1000) for 2 h at room temperature. The coverslips were washed with PBT and then incubated with secondary antibodies diluted in blocking buffer. Secondary antibodies used were rhodamine (TRITC) donkey antirat IgG (Jackson 712-026-150, diluted 1:300) and Alexa Fluor 488 antirabbit IgG (Moleular Probes A11008, diluted 1:300) for 1 h at room temperature. Coverslips were washed with PBT, incubated for 30 s in PBS containing 0.5 μg/mL DAPI, and then mounted.

Supporting Information Available: Figure 1 showing kinase inhibitory activity of compound **18**; Figure 2 showing activity of compound **18** in tumor models; synthesis and characterization of compounds **7h**, **11−17**, and **19−24**; experimental details for biopharmaceutical profiling, rat pharmacokinetics, cell viability assay, murine P388/D1 leukemia model, NCI-H460 xenograft, X-ray crystallography, and molecular modeling. This material is available free of charge via the Internet at http://pubs.acs.org.

References

(1) Barr, A. R.; Gergely, F. Aurora-A: the maker and breaker of spindle poles. *J. Cell Sci.* **2007**, *120*, 2987–2996.

(2) Carmena, M.; Ruchaud, S.; Earnshaw, W. C. Making the auroras glow: regulation of aurora A and B kinase function by interacting proteins. *Curr. Opin. Cell Biol.* **2009**, *21*, 796–805.

(3) Yan, X.; Cao, L.; Li, Q.; Wu, Y.; Zhang, H.; Saiyin, H.; Liu, X.; Zhang, X.; Shi, Q.; Yu, L. Aurora C is directly associated with survivin and required for cytokinesis. *Genes Cells* **2005**, *10*, 617–626.

(4) Gautschi, O.; Heighway, J.; Mack, P. C.; Purnell, P. R.; Lara, P. N., Jr.; Gandara, D. R. Aurora kinases as anticancer drug targets. *Clin. Cancer Res.* **2008**, *14*, 1639–1648.

(5) Mountzios, G.; Terpos, E.; Dimopoulos, M. A. Aurora kinases as targets for cancer therapy. *Cancer Treat. Rev.* **2008**, *34*, 175–182.

(6) Bischoff, J. R.; Anderson, L.; Zhu, Y.; Mossie, K.; Ng, L.; Souza, B.; Schryver, B.; Flanagan, P.; Clairvoyant, F.; Ginther, C.; Chan, C. S.; Novotny, M.; Slamon, D. J.; Plowman, G. D. A homologue of Drosophila aurora kinase is oncogenic and amplified in human colorectal cancers. *EMBO J.* **1998**, *17*, 3052–3065.

(7) Bischoff, J. R.; Plowman, G. D. The aurora/Ipl1p kinase family: regulators of chromosome segregation and cytokinesis. *Trends Cell Biol.* **1999**, *9*, 454–459.

(8) Ke, Y. W.; Dou, Z.; Zhang, J.; Yao, X. B. Function and regulation of aurora/Ipl1p kinase family in cell division. *Cell Res.* **2003**, *13*, 69–81.

(9) Katayama, H.; Sasai, K.; Kawai, H.; Yuan, Z.-M.; Bondaruk, J.; Suzuki, F.; Fujii, S.; Arlinghaus, R. B.; Czerniak, B. A.; Sen, S. Phosphorylation by aurora kinase A induces Mdm2-mediated destabilization and inhibition of p53. *Nat. Genet.* **2004**, *36*, 55–62.

(10) Zhang, D.; Hirota, T.; Marumoto, T.; Shimizu, M.; Kunitoku, N.; Sasayama, T.; Arima, Y.; Feng, L.; Suzuki, M.; Takeya, M.; Saya, H. Cre-loxP-controlled periodic aurora-A overexpression induces mitotic abnormalities and hyperplasia in mammary glands of mouse models. *Oncogene* **2004**, *23*, 8720–8730.

(11) Fu, J.; Bian, M.; Jiang, Q.; Zhang, C. Roles of aurora kinases in mitosis and tumorigenesis. *Mol. Cancer Res.* **2007**, *5*, 1–10.

(12) Anand, S.; Penrhyn-Lowe, S.; Venkitaraman, A. R. AURORA-A amplification overrides the mitotic spindle assembly checkpoint, inducing resistance to Taxol. *Cancer Cell* **2003**, *3*, 51–62.

(13) Hata, T.; Furukawa, T.; Sunamura, M.; Egawa, S.; Motoi, F.; Ohmura, N.; Marumoto, T.; Saya, H.; Horii, A. RNA interference targeting aurora kinase a suppresses tumor growth and enhances the taxane chemosensitivity in human pancreatic cancer cells. *Cancer Res.* **2005**, *65*, 2899–2905.

(14) Ota, T.; Suto, S.; Katayama, H.; Han, Z. B.; Suzuki, F.; Maeda, M.; Tanino, M.; Terada, Y.; Tatsuka, M. Increased mitotic phosphorylation of histone H3 attributable to AIM-1/aurora-B overexpression contributes to chromosome number instability. *Cancer Res.* **2002**, *62*, 5168–5177.

(15) Hontz, A. E.; Li, S. A.; Lingle, W. L.; Negron, V.; Bruzek, A.; Salisbury, J. L.; Li, J. J. Aurora A and B overexpression and centrosome amplification in early estrogen-induced tumor foci in the Syrian hamster kidney: implications for chromosomal instability, aneuploidy, and neoplasia. *Cancer Res.* **2007**, *67*, 2957–2963.

(16) Smith, S. L.; Bowers, N. L.; Betticher, D. C.; Gautschi, O.; Ratschiller, D.; Hoban, P. R.; Booton, R.; Santibanez-Koref, M. F.; Heighway, J. Overexpression of aurora B kinase (AURKB) in primary non-small cell lung carcinoma is frequent, generally driven from one allele, and correlates with the level of genetic instability. *Br. J. Cancer* **2005**, *93*, 719–729.

(17) Keen, N.; Taylor, S. Aurora-kinase inhibitors as anticancer agents. *Nat. Rev. Cancer* **2004**, *4*, 927–936.

(18) Hirota, T.; Kunitoku, N.; Sasayama, T.; Marumoto, T.; Zhang, D.; Nitta, M.; Hatakeyama, K.; Saya, H. Aurora-A and an interacting activator, the LIM protein Ajuba, are required for mitotic commitment in human cells. *Cell* **2003**, *114*, 585–598.

(19) Meraldi, P.; Honda, R.; Nigg, E. A. Aurora kinases link chromosome segregation and cell division to cancer susceptibility. *Curr. Opin. Genet. Dev.* **2004**, *14*, 29–36.

(20) Kallio, M. J.; McCleland, M. L.; Stukenberg, P. T.; Gorbsky, G. J. Inhibition of aurora B kinase blocks chromosome segregation, overrides the spindle checkpoint, and perturbs microtubule dynamics in mitosis. *Curr. Biol.* **2002**, *12*, 900–905.

(21) Warner, S. L.; Munoz, R. M.; Stafford, P.; Koller, E.; Hurley, L. H.; Von Hoff, D. D.; Han, H. Comparing aurora A and aurora B as molecular targets for growth inhibition of pancreatic cancer cells. *Mol. Cancer Ther.* **2006**, *5*, 2450–2458.

(22) Manfredi, M. G.; Ecsedy, J. A.; Meetze, K. A.; Balani, S. K.; Burenkova, O.; Chen, W.; Galvin, K. M.; Hoar, K. M.; Huck, J. J.; LeRoy, P. J.; Ray, E. T.; Sells, T. B.; Stringer, B.; Stroud, S. G.; Vos, T. J.; Weatherhead, G. S.; Wysong, D. R.; Zhang, M.; Bolen, J. B.; Claiborne, C. F. Antitumor activity of MLN8054, an orally active small-molecule inhibitor of aurora A kinase. *Proc. Natl. Acad. Sci. U.S.A.* **2007**, *104*, 4106–4111.

(23) Yang, H.; Burke, T.; Dempsey, J.; Diaz, B.; Collins, E.; Toth, J.; Beckmann, R.; Ye, X. Mitotic requirement for aurora A kinase is bypassed in the absence of aurora B kinase. *FEBS Lett.* **2005**, *579*, 3385–3391.

(24) Pollard, J. R.; Mortimore, M. Discovery and development of aurora kinase inhibitors as anticancer agents. *J. Med. Chem.* **2009**, *52*, 2629–2651.

(25) Hauf, S.; Cole, R. W.; LaTerra, S.; Zimmer, C.; Schnapp, G.; Walter, R.; Heckel, A.; Meel, J. v.; Rieder, C. L.; Peters, J.-M. The small molecule hesperadin reveals a role for aurora B in correcting kinetochore−microtubule attachment and in maintaining the spindle assembly checkpoint. *J. Cell Biol.* **2003**, *161*, 281–294.

(26) Ditchfield, C.; Johnson, V. L.; Tighe, A.; Ellston, R.; Haworth, C.; Johnson, T.; Mortlock, A.; Keen, N.; Taylor, S. S. Aurora B couples chromosome alignment with anaphase by targeting BubR1, Mad2, and Cenp-E to kinetochores. *J. Cell Biol.* **2003**, *161*, 267–280.

(27) Wang, Y.; Serradell, N. VX-680/MK-0457 aurora kinase inhibitor oncolytic. *Drugs Future* **2007**, *32*, 144–147.

(28) Gontarewicz, A.; Brummendorf, T. H. Danusertib (formerly PHA-739358)—a novel combined pan-aurora kinases and third generation Bcr-Abl tyrosine kinase inhibitor. *Recent Results Cancer. Res.* **2010**, *184*, 199–214.

(29) Carpinelli, P.; Ceruti, R.; Giorgini, M. L.; Cappella, P.; Gianellini, L.; Croci, V.; Degrassi, A.; Texido, G.; Rocchetti, M.; Vianello, P.; Rusconi, L.; Storici, P.; Zugnoni, P.; Arrigoni, C.; Soncini, C.; Alli, C.; Patton, V.; Marsiglio, A.; Ballinari, D.; Pesenti, E.; Fancelli, D.; Moll, J. PHA-739358, a potent inhibitor of aurora kinases with a selective target inhibition profile relevant to cancer. *Mol. Cancer Ther.* **2007**, *6*, 3158–3168.

(30) Harrington, E. A.; Bebbington, D.; Moore, J.; Rasmussen, R. K.; Ajose-Adeogun, A. O.; Nakayama, T.; Graham, J. A.; Demur, C.; Hercend, T.; Diu-Hercend, A.; Su, M.; Golec, J. M. C.; Miller, K. M. VX-680, a potent and selective small-molecule inhibitor of the aurora kinases, suppresses tumor growth in vivo. *Nat. Med.* **2004**, *10*, 262–267.

(31) Warner, S. L.; Bashyam, S.; Vankayalapati, H.; Bearss, D. J.; Han, H.; Von Hoff, D. D.; Hurley, L. H. Identification of a lead small-molecule inhibitor of the aurora kinases using a structure-assisted, fragment-based approach. *Mol. Cancer Ther.* **2006**, *5*, 1764–1773.

(32) Wilkinson, R. W.; Odedra, R.; Heaton, S. P.; Wedge, S. R.; Keen, N. J.; Crafter, C.; Foster, J. R.; Brady, M. C.; Bigley, A.; Brown, E.; Byth, K. F.; Barrass, N. C.; Mundt, K. E.; Foote, K. M.; Heron, N. M.; Jung, F. H.; Mortlock, A. A.; Boyle, F. T.; Green, S. AZD1152, a selective inhibitor of aurora B kinase, inhibits human tumor xenograft growth by inducing apoptosis. *Clin. Cancer Res.* **2007**, *13*, 3682–3688.

(33) Hoar, K.; Chakravarty, A.; Rabino, C.; Wysong, D.; Bowman, D.; Roy, N.; Ecsedy, J. A. MLN8054, a small-molecule inhibitor of aurora A, causes spindle pole and chromosome congression defects leading to aneuploidy. *Mol. Cell. Biol.* **2007**, *27*, 4513–4525.

(34) Kontopidis, G.; McInnes, C.; Pandalaneni, S. R.; McNae, I.; Gibson, D.; Mezna, M.; Thomas, M.; Wood, G.; Wang, S.; Walkinshaw, M. D.; Fischer, P. M. Differential binding of inhibitors to active and inactive CDK2 provides insights for drug design. *Chem. Biol.* **2006**, *13*, 201–211.

(35) McInnes, C.; Wang, S.; Anderson, S.; O'Boyle, J.; Jackson, W.; Kontopidis, G.; Meades, C.; Mezna, M.; Thomas, M.; Wood, G.; Lane, D. P.; Fischer, P. M. Structural determinants of CDK4 inhibition and design of selective ATP competitive inhibitors. *Chem. Biol.* **2004**, *11*, 525–534.

(36) Wang, S.; Meades, C.; Wood, G.; Osnowski, A.; Anderson, S.; Yuill, R.; Thomas, M.; Mezna, M.; Jackson, W.; Midgley, C.; Griffiths, G.; Fleming, I.; Green, S.; McNae, I.; Wu, S.-Y.; McInnes, C.; Zheleva, D.; Walkinshaw, M. D.; Fischer, P. M. 2-Anilino-4-(thiazol-5-yl)pyrimidine CDK inhibitors: synthesis,

(37) Wang, S.; Wood, G.; Meades, C.; Griffiths, G.; Midgley, C.; McNae, I.; McInnes, C.; Anderson, S.; Jackson, W.; Mezna, M.; Yuill, R.; Walkinshaw, M.; Fischer, P. M. Synthesis and biological activity of 2-anilino-4-(1*H*-pyrrol-3-yl)pyrimidine CDK inhibitors. *Bioorg. Med. Chem. Lett.* **2004**, *14*, 4237–4240.

(38) Wu, S. Y.; McNae, I.; Kontopidis, G.; McClue, S. J.; McInnes, C.; Stewart, K. J.; Wang, S.; Zheleva, D. I.; Marriage, H.; Lane, D. P.; Taylor, P.; Fischer, P. M.; Walkinshaw, M. D. Discovery of a novel family of CDK inhibitors with the program LIDAEUS: structural basis for ligand-induced disordering of the activation loop. *Structure* **2003**, *11*, 399–410.

(39) Griffiths, G.; Midgley, C.; Grabarek, J.; Cooper, M.; Glover, D.; Ingram, L.; Jackson, W.; Meades, C.; Mezna, M.; O'Boyle, J.; Wood, G.; Yuill, R.; Lane, D. P.; Jackson, R.; Fischer, P. M.; Wang, S. Identification and characterization of kinase inhibitors that inhibit CDK2, CDK7 and CDK 9 activities, induce p53 and result in reduced proliferation and induction of apoptosis of human tumor cells. *Proc. Am. Assoc. Cancer Res.* **2004**, *45*, Abstract 837.

(40) Wang, S.; Wood, G.; Meades, C.; Griffiths, G.; Midgley, C.; Grabarek, J.; Cooper, M.; Anderson, S.; Jackson, W.; Yuill, R.; McNae, I.; McInnes, C.; Zheleva, D.; Walkinshaw, M.; Lane, D. P.; Jackson, R.; Fischer, P. M. Discovery of 2-phenylamino-4-(pyrrol-3-yl)-pyrimidines new class of CDK inhibitors: synthesis, crystal structures, in vitro anti-proliferative activity and biochemical evaluation. *Clin. Cancer Res.* **2003**, *9* (16, Suppl.), Abstract C61.

(41) Bredereck, H.; Effenberger, F.; Botsch, H. Acid amide reactions. XLV. Reactivity of formamidines, dimethylformamide diethyl acetal (amide acetal), and bis(dimethylamino)methoxymethane (aminal ester). *Chem. Ber.* **1964**, *97*, 3397–3406.

(42) Orus, L.; Martinez, J.; Perez, S.; Oficialdegui, A. M.; del Castillo, J. C.; Mourelle, M.; Lasheras, B.; del Rio, J.; Monge, A. New 3-[4-(3-substituted phenyl)piperazin-1-yl]-l-(benzo[*b*]thiophen-3-yl)-propanol derivatives with dual action at 5-HT1A serotonin receptors and serotonin transporter as a new class of antidepressants. *Pharmazie* **2002**, *57*, 515–518.

(43) Zhai, S.; Senderowicz, A.; Sausville, E. A.; Figg, W. D. Flavopiridol, a novel cyclin-dependent kinase inhibitor, in clinical development. *Ann. Pharmacother.* **2002**, *36*, 905–911.

(44) Wang, S.; McClue, S. J.; Ferguson, J. R.; Hull, J. D.; Stokes, S.; Parsons, S.; Westwood, R.; Fischer, P. M. Synthesis and configuration of the cyclin-dependent kinase inhibitor roscovitine and its enantiomer. *Tetrahedron: Asymmetry* **2001**, *12*, 2891–2894.

(45) Fischer, P. M. The use of CDK inhibitors in oncology: a pharmaceutical perspective. *Cell Cycle* **2004**, *3*, 742–746.

(46) Lu, W.; Chen, L.; Peng, Y.; Chen, J. Activation of p53 by roscovitine-mediated suppression of MDM2 expression. *Oncogene* **2001**, *20*, 3206–3216.

(47) Ljungman, M.; Paulsen, M. T. The cyclin-dependent kinase inhibitor roscovitine inhibits RNA synthesis and triggers nuclear accumulation of p53 that is unmodified at Ser15 and Lys382. *Mol. Pharmacol.* **2001**, *60*, 785–789.

(48) Juan, G.; Traganos, F.; James, W. M.; Ray, J. M.; Roberge, M.; Sauve, D. M.; Anderson, H.; Darzynkiewicz, Z. Histone H3 phosphorylation and expression of cyclins A and B1 measured in individual cells during their progression through G2 and mitosis. *Cytometry* **1998**, *32*, 71–77.

(49) Gasparri, F.; Mariani, M.; Sola, F.; Galvani, A. Quantification of the proliferation index of human dermal fibroblast cultures with the ArrayScan high-content screening reader. *J. Biomol. Screening* **2004**, *9*, 232–243.

(50) Gillespie, D. A.; Walker, M. Mitotic index determination by flow cytometry. *Subcell. Biochem.* **2006**, *40*, 355–358.

(51) Davis, F. M.; Tsao, T. Y.; Fowler, S. K.; Rao, P. N. Monoclonal antibodies to mitotic cells. *Proc. Natl. Acad. Sci. U.S.A.* **1983**, *80*, 2926–2930.

(52) Crosio, C.; Fimia, G. M.; Loury, R.; Kimura, M.; Okano, Y.; Zhou, H.; Sen, S.; Allis, C. D.; Sassone-Corsi, P. Mitotic phosphorylation of histone H3: spatio-temporal regulation by mammalian aurora kinases. *Mol. Cell. Biol.* **2002**, *22*, 874–885.

(53) Pascreau, G.; Arlot-Bonnemains, Y.; Prigent, C. Phosphorylation of histone and histone-like proteins by aurora kinases during mitosis. *Prog. Cell Cycle Res.* **2003**, *5*, 369–374.

(54) Ikezoe, T. Aurora kinases as an anti-cancer target. *Cancer Lett.* **2008**, *262*, 1–9.

(55) Giet, R.; McLean, D.; Descamps, S.; Lee, M. J.; Raff, J. W.; Prigent, C.; Glover, D. M. Drosophila aurora A kinase is required to localize D-TACC to centrosomes and to regulate astral microtubules. *J. Cell Biol.* **2002**, *156*, 437–451.

(56) Giet, R.; Glover, D. M. Drosophila aurora B kinase is required for histone H3 phosphorylation and condensin recruitment during

chromosome condensation and to organize the central spindle during cytokinesis. *J. Cell Biol.* **2001**, *152*, 669–682.

(57) Glover, D. M.; Leibowitz, M. H.; McLean, D. A.; Parry, H. Mutations in aurora prevent centrosome separation leading to the formation of monopolar spindles. *Cell* **1995**, *81*, 95–105.

(58) Avdeef, A. pH-metric log P. II. Refinement of partition coefficients and ionization constants of multiprotic substances. *J. Pharm. Sci.* **1993**, *82*, 183–190.

(59) Li, A. P. Screening for human ADME/Tox drug properties in drug discovery. *Drug Discovery Today* **2001**, *6*, 357–366.

(60) Tarbit, M. H.; Berman, J. High-throughput approaches for evaluating absorption, distribution, metabolism and excretion properties of lead compounds. *Curr. Opin. Chem. Biol.* **1998**, *2*, 411–416.

(61) Haselsberger, K.; Peterson, D. C.; Thomas, D. G.; Darling, J. L. Assay of anticancer drugs in tissue culture: comparison of a tetrazolium-based assay and a protein binding dye assay in short-term cultures derived from human malignant glioma. *Anti-Cancer Drugs* **1996**, *7*, 331–338.

(62) Levis, M.; Allebach, J.; Tse, K. F.; Zheng, R.; Baldwin, B. R.; Smith, B. D.; Jones-Bolin, S.; Ruggeri, B.; Dionne, C.; Small, D. A FLT3-targeted tyrosine kinase inhibitor is cytotoxic to leukemia cells in vitro and in vivo. *Blood* **2002**, *99*, 3885–3891.

(63) He, Q.; Huang, Y.; Sheikh, M. S. Proteasome inhibitor MG132 upregulates death receptor 5 and cooperates with Apo2L/TRAIL to induce apoptosis in Bax-proficient and -deficient cells. *Oncogene* **2004**, *23*, 2554–2558.

(64) Bayliss, R.; Sardon, T.; Vernos, I.; Conti, E. Structural basis of aurora-A activation by TPX2 at the mitotic spindle. *Mol. Cell* **2003**, *12*, 851–862.

(65) Eyers, P. A.; Erikson, E.; Chen, L. G.; Maller, J. L. A novel mechanism for activation of the protein kinase aurora A. *Curr. Biol.* **2003**, *13*, 691–697.

(66) Yasui, Y.; Urano, T.; Kawajiri, A.; Nagata, K.; Tatsuka, M.; Saya, H.; Furukawa, K.; Takahashi, T.; Izawa, I.; Inagaki, M. Autophosphorylation of a newly identified site of aurora-B is indispensable for cytokinesis. *J. Biol. Chem.* **2004**, *279*, 12997–13003.

(67) Marsh, J. C.; Shoemaker, R. H.; Suffness, M. Stability of the in vivo P388 leukemia model in evaluation of antitumor activity of natural products. *Cancer Treat. Rep.* **1985**, *69*, 683–685.

(68) Griffiths, G.; Scaerou, F.; Midgley, C.; McClue, S.; Tosh, C.; Jackson, W.; MacCallum, D.; Wang, S.; Fischer, P.; Glover, D.; Zheleva, D. Anti-tumor activity of CYC116, a novel small molecule inhibitor of aurora kinases and VEGFR2. *Proc. Am. Assoc. Cancer Res.* **2008**, *49*, Abstract 5644.

(69) Hajduch, M.; Vydra, D.; Dzubak, P.; Dziechciarkova, M.; Stuart, I.; Zheleva, D. In vivo mode of action of CYC116, a novel small molecule inhibitor of aurora kinases and VEGFR2. *Proc. Am. Assoc. Cancer Res.* **2008**, *49*, Abstract 5645.

(70) Still, W. C.; Kahn, M.; Mitra, A. Rapid chromatographic technique for preparative separations with moderate resolution. *J. Org. Chem.* **1978**, *43*, 2923–2925.

(71) Cheng, Y.-C.; Prusoff, W. H. Relation between the inhibition constant (IK1) and the concentration of inhibitor which causes fifty per cent inhibition (I50) of an enzymic reaction. *Biochem. Pharmacol.* **1973**, *22*, 3099–3108.

(72) Sessa, F.; Mapelli, M.; Ciferri, C.; Tarricone, C.; Areces, L. B.; Schneider, T. R.; Stukenberg, P. T.; Musacchio, A. Mechanism of aurora B activation by INCENP and inhibition by hesperadin. *Mol. Cell* **2005**, *18*, 379–391.

(73) Midgley, C. A.; Fisher, C. J.; Bartek, J.; Vojtesek, B.; Lane, D.; Barnes, D. M. Analysis of p53 expression in human tumors: an antibody raised against human p53 expressed in *Escherichia coli*. *J. Cell Sci.* **1992**, *101*, 183–189.